Jundishapur J Nat Pharm Prod. 2020 May; 15(2):e91886. doi: 10.5812/jjnpp.91886.

Published online 2020 January 21. **Research Article**

Synthesis and Investigation of the Curcumin-Loaded Magnetic Lipid Nanoparticles and Their Cytotoxicity Assessment on Human Breast Carcinoma Cell Line

Somayeh Karami [1], Kobra Rostamizadeh [2], Nasim Shademani [3] and Maliheh Parsa [4, *]

[1] School of Pharmacy, Zanjan University of Medical Sciences, Zanjan, Iran
[2] Zanjan Pharmaceutical Nanotechnology Research Center (ZPNRC), Department of Pharmaceutical Biomaterial, Zanjan University of Medical Sciences, Zanjan, Iran
[3] Zanjan Pharmaceutical Nanotechnology Research Center (ZPNRC), Zanjan University of Medical Sciences, Zanjan, Iran
[4] Department of Toxicology and Pharmacology, Faculty of Pharmacy, Zanjan University of Medical Sciences, Zanjan, Iran

[*] *Corresponding author*: Department of Toxicology and Pharmacology, Faculty of Pharmacy, Zanjan University of Medical Sciences, Zanjan, Iran. Tel: +98-9177328524, Email: parsa@zums.ac.ir

Received 2019 March 30; **Revised** 2019 June 14; **Accepted** 2019 July 17.

Abstract

Chemotherapy fails to eradicate cancer cells, mainly due to the lack of selective drug accumulation into the tumor site, which can affect healthy cells, as well. In this research, we studied the magnetite nanostructured lipid carriers (NLCs) for targeted delivery of curcumin into breast cancer cells. Superparamagnetic iron oxide nanoparticles (SPIONs) were prepared using coprecipitation method by mixing $FeCl_2$ and $FeCl_3$ in a suitable ratio in alkaline media. The resultant ferrofluid was very stable and possessed high magnetic properties. To prepare SPIONs containing NLCs (NLC-SPIONs), cetyl palmitate and cod-liver oil, Tween 80 and span60 were used as solid lipid, liquid lipid, surfactant, and co-surfactant, respectively. Curcumin as an anticancer drug was loaded into NLC-SPIONs (CUR-NLC-SPIONs) and its characteristics, including particle size, zeta potential, polydispersity index (PDI), drug entrapment efficacy, drug-loading capacity, and thermal stability were evaluated. The results showed that CUR-NLC-SPIONs had a mean particle size of 166.7 $\pm$ 14.20 nm, mean zeta potential of -27.6 $\pm$ 3.83 mv, and PDI of 0.24 $\pm$ 0.14. Encapsulation efficiency for all prepared nanoparticles (NPs) was 99.95 $\pm$ 0.015% and drug-loading capacity was 3.76 $\pm$ 0.005%. Morphological studies were carried out by transmission electron microscopy (TEM) indicating spherical morphology of the NPs. 3-(4,5-dimethylthiazol-2-yl)-2,5-diphenyltetrazolium bromide (MTT) assay measurements on cell viability proved that the synthesized CUR-NLC-SPIONs possess a better cytotoxic activity against human breast cancer cells compared with free curcumin. This new drug delivery system, which benefits from superparamagnetic properties may serve as a suitable platform for developing new biocompatible drug carriers and with a potential to use in targeted cancer therapy.

Keywords: Cancer, Superparamagnetic, Nanostructure Lipid Carrier, Curcumin, Targeted Drug Delivery

1. Background

Breast cancer is the second reason for cancer-related death in women worldwide (1). In 2016, a total of 246,660 new cases of breast cancer and 14% of deaths due to breast cancer were reported in the US (2). Chemotherapy is considered as the most frequent systemic treatment for suppressing the tumor cell proliferation and subsequent disease progression and metastasis. However, chemotherapeutic agents not only kill tumor cells, but also deleteriously affect normal cells. Therefore, anti-cancer drug carriers characterized by targeted cancer therapy on cancer cells without affecting normal cells to maintain or improve the efficacy of drug delivery and reduce the burden of adverse reactions and side effects are urgently needed. To address this issue, a promising approach is using drug-delivery systems, of which nanosized drug-carrier systems have especially been interested (3). NPs, due to the different biological properties and applicability in a wide range of settings, provide a safe and effective platform for targeted-delivery systems of chemotherapeutic agents. These systems are classified into two main groups: polymeric nanoparticles and lipid nanoparticles (LNPs). LNPs, due to their natural and biological origins, are less toxic than polymeric NPs. Nanostructured lipid carriers (NLCs) are the second generation of LNPs after solid LNPs, which benefit from the advantages of both nanoemulsion and solid NPs. They can also be easily synthesized with oil-in-water nanoemulsion (4).

In targeted therapy, the development of magnetically

guided drug delivery systems has widely considered (3), since it allows directing magnetic NPs to be concentrated at a target region by a simple external magnetic field. The characteristics, such as biocompatibility, non-toxicity, small size, magnetization, a high degree of saturation, and ease of appropriate surface modification with different polymers have made superparamagnetic iron oxide nanoparticles (SPIONs), especially those containing magnetite (Fe_3O_4), as the best choice for site-specific drug delivery systems (3).

Several studies have recently evaluated magnetic NPs loaded with different drugs (5, 6). For example, Cicha et al. (7) evaluated mitoxantrone-carrying SPIONs and the drug released from SPIONs. Mancarella et al. (8) developed a layer-by-layer functionalization of Fe_3O_4 NPs by coating them in dextran and poly-L-lysine. The results showed a high percentage of curcumin loaded Fe_3O_4 NPs for treating ovarian cancer (8).

Curcumin is a natural hydrophobic diphenol derived from the rhizomes of plant *Curcuma longa*. Numerous studies have confirmed the potential of curcumin in prevention and treatment of various cancer types, such as head and neck, melanoma, colon, breast, pancreatic, prostate, and ovarian cancers. The multiple molecular targeting of curcumin to selectively kill tumor cells with low intrinsic toxicity has been demonstrated in different studies (9-11). However, the properties, such as a high hydrophobicity, instability, and poor bioavailability limit its further clinical use (12). Therefore, there is a need for finding new strategies to improve the physicochemical properties and therapeutic efficacy of curcumin. Curcumin-loaded magnetic NLCs, along with oleic acid as a stabilizer, may provide a novel approach for use in the treatment of different cancers (13).

2. Objectives

The aim of the present study was to synthesize the SPIONs and combine them with NLC for the curcumin entrapment and evaluate their features in human breast carcinoma cell line. In our knowledge, this is the first study, which combined the features of NLC and SPIONs to targeted delivery of curcumin.

3. Methods

3.1. Material

Curcumin, $FeCl_3$ and $FeCl_2$ were purchased from the Merck Chemicals (Germany). Cetylpalmitate was received as a gift from the Alborz Bulk Pharmaceutical Co. Fish oil was purchased from the Daana Pharma Co. (Tehran, Iran). In addition, 3-(4,5-dimethylthiazol-2-yl)-2,5-diphenyltetrazolium bromide 17 (MTT) powder and Roswell Park Memorial Institute (1640) Medium were obtained from the ATOCell Co. (Hungry). Fetal bovine serum (FBS) and trypsin-EDTA 10 × were obtained from the Biosera Co. (England). Dimethylsulfoxide (DMSO), ethanol, dichloromethane, Tween 80 and Span 60 were also obtained from the Merck Co. MCF-7 cells were purchased from the NCBI-National Cell Bank of the Pasteur Institute (Iran).

3.2. Synthesis of SPIONs

Chemical synthesis of SPIONs was performed by co-precipitation reaction of Fe^{3+}/Fe^{2+}in aqueous form (14). $FeCl_3$ (0.5 g) and $FeCl_2$ (0.29 g) with the molar proportion of 2:1 were dissolved in deionized water (45 mL) and maintained at 80°C temperatures in an inert nitrogen atmosphere of nitrogen and alkaline medium. Then, ammonia solution (5 mL) was gradually added into the mixture to obtain the final pH of 11. The oleic acid (5 - 6 drops) was added into the suspensions and stirred for 30 min. The black precipitated particles were magnetically separated and washed two times with deionized water and one time with acetone to remove the extra ammonium. The products were then dried at 60°C in an oven for 24 h.

3.3. Preparation of the NLC-SPIOINs Loaded with Curcumin (CUR-NLC-SPIONs)

CUR-NLC-SPIONs were prepared by homogenization technique, as described by Hsu et al. with some modification (15). Briefly, the lipid phase was produced by mixing dichloromethane (12 mL) and Fe_3O_4 NPs (5 mg) and subsequent ultrasonication at room temperature for 10 - 15 min to completely disperse the NPs. When Fe_3O_4 particles were completely dispersed, the clear and transparent solution changed to a black suspension. Then, curcumin, fish oil (liquid lipid, 200 mg) and cetylpalmitate (solid lipid, 250 mg) were added to this mixture. The aqueous phase consisting of Tween 80 (150 mg) and span 60 (150 mg) surfactants in deionized water was heated to the temperature of 70°C for 5 - 10 min on a stirrer. After that, the hot oil phase was gradually added to the aqueous phase under constant stirring at 10000 rpm for 5 - 6 min followed by further homogenization for 10 min at 13000 rpm. Finally, the resultant suspension was allowed to cool down at room temperature, leading to forming the CUR-NLC-SPIONs.

3.4. Characterization of the NPs

3.4.1. Particle Size and Distribution

The particle size, distribution, and zeta potential of the CUR-NLC-SPIONs were measured by dynamic light scattering (DLS) using a Zeta sizer device coupled with a He-Ne

laser at a temperature of ± 25°C. The measurements were performed at a scattering angle of 173°. Prior to measurements, samples were diluted with deionized water to eliminate viscosity and generate appropriate scattering intensity, which confirmed by the absorbance at 633 nm. Three independent measurements in 3 consequent days were recorded for NPs.

3.4.2. Transmission Electron Microscopy (TEM)

The size and morphology of SPIONs and CUR-NLC-SPIONs were further studied by transmission electron microscopy (TEM) using the negative-staining method. A diluted sample of CUR-NLC-SPIONs was stained with phosphotungstic acid and applied on carbon-coated Cu grid and allowed to dry. Then, the grid was observed by TEM.

3.5. Stability of CUR-NLC-SPIONs

To determine the stability of each prepared formulation, the samples were stored at three different temperatures of 25°C, 4°C, and 45°C for 5 months (16). During this period, samples were withdrawn from the stock solution on days 1, 3, 7, 14, 21, and 30 and then every month up to 5 months to determine zeta potential, size, and distribution. For every formulation, three samples were used.

3.6. Entrapment Efficiency and Drug Loading Capacity

The drug loading capacity and entrapment efficiency of CUR-NLC-SPIONs were determined by measuring the amount of free drug in the dispersion medium using ultrafiltration technique (17). In this regard, 3 mL of the formulation was poured in the Amicon device and centrifuged for 20 min at 4000 rpm to separate the NPs. Next, the supernatant containing free unloaded drug was analyzed by UV spectrophotometer at 426 nm. Entrapment efficiency was calculated using the Equation 1. The standard calibration curve for curcumin was obtained by measuring different concentrations of curcumin in ethanol. The percent of drug loading was calculated using the reverse method using the Equations 1 and 2. The accuracy and precision (relative standard deviation, %) and sensitivity (limit of detection) of used tests were also calculated.

$$Entrapment\ Efficency,\ \% = \frac{Total\ drug - Free\ drug}{Total\ drug} \times 100 \quad (1)$$

$$Drug\ Loading,\ \% = \frac{Total\ drug - Free\ drug}{Total\ lipids} \times 100 \quad (2)$$

3.7. Drug Release Study

The in vitro measurements of drug release from CUR-NLC-SPIONs were carried out using dialysis sack and phosphate-buffered saline (PBS) containing 30% ethanol (pH = 7.4) as receptor compartment. Then, 1 mL of each formulation was poured in dialysis membrane immersed in 19 mL of PBS and the system was maintained at 37°C under continuous stirring. At predetermined time intervals, 2 mL of the sample was withdrawn from PBS and replaced with fresh PBS/ethanol solution. The drug concentration in the receptor compartment was measured at 426 nm using UV spectrophotometer. The standard calibration curve for curcumin was obtained by measuring different concentrations of curcumin in the receptor compartment medium. To ensure that constant drug release is not due to the membrane, curcumin alone, dispersed in the same concentration, was studied under the same condition for release. The released amount was calculated again by data obtained by UV spectrophotometer. Calculation of the concentration of the released curcumin was performed using a valid calibration curve.

3.8. Cell Viability Assay

The cytotoxicity of the various formulations, including free NLC-SPIONs and CUR-NLC-SPIONs were estimated using MTT assay (18). Briefly, MCF-7 cells were grown in the RPMI-1640 medium supplemented with 10% FBS and 1% penicillin/streptomycin and incubated in a humidified cell culture incubator with 95% O_2 and 5% CO_2 atmosphere. The confluent monolayer cells were harvested with trypsin/EDTA from T-75 cell culture flasks and seeded into 96-well microplates at a density of 104 cells/well and were exposed to the 10, 50, and 100 mg/mL of SPOIN-NLC and SPOIN-NLC-curcumin for 24, 48, 72, and 96 h. After passing the desired exposure time, cell viabilities were estimated using MTT assay. Briefly, 5 mg/mL of the MTT solution was added to the plates and incubated for 4 h. Thereafter, purple formazan crystals were dissolved with DMSO and the absorbance was read at 570 nm and 690 nm as the reference. Cell viability was reported as the percentage of viable cells compared with the control group.

4. Results

4.1. TEM Results for SPIONs and CUR-NLC-SPIONs

TEM was performed to evaluate the morphology and distribution of the SPIONSs, as well as CUR-NLC-SPIONs. As can be seen in Figure 1A, all the SPIONs showed a homogeneously spherical shape with a diameter of about 8 - 10

nm, which is consistent with the results of the other studies (19). Figure 2B illustrates the TEM image of CUR-NLC-SPIONs indicating the size of these particles at the range of 100 - 150 nm, which is consistent with DLS results (20, 21).

4.2. Particle Size, Distribution and Zeta Potential of SPIONs and CUR-NLC-SPIONs

DLS was carried out as a next method to determine the particle size and distribution of SPIONs and CUR-NLC-SPIONs, as shown in Figure 2. The mean size of SPIONs and CUR-NLC-SPIONs were obtained 209.6 $\pm$ 18.91 and 166.7 $\pm$ 14.20 nm, respectively. The results of CUR-NLC-SPIONs were consistent with the size range obtained by TEM with very slight differences. However, regarding SPIONs, a significant difference was found. PDI for SPIONs and CUR-NLC-SPIONs was found 0.22 $\pm$ 0.02 and 0.24 $\pm$ 0.14, respectively, which is in an acceptable range (22), showing the desired distribution for these particles (Figure 2A and C). Zeta potential is indicative of the particle surface charge and is a determinant parameter for instability of NPs. According to the results, the zeta potential was found -25.4 $\pm$ 2.77 mV and -27.6 $\pm$ 3.83 mV for CUR-NLS-SPIONs and SPIONs, respectively (Figure 2B and D). The negative charge of SPIONs is attributed to the formation of carboxylate ions of oleic acid decorated on the outer surface of MNPs (23). An increase in surface charge of SPIONs It is believed that the minimum zeta potential of $\pm$ 30 mV can provide an adequate stability for NPs (24). Therefore, considering the obtained zeta potential for both particles, a good stability was expected for them.

4.3. Physical Stability of CUR-NLC-SPIONs

To determine the stability of CUR-NLC-SPIONs, the samples were placed at three temperatures of 25°C, 4°C, and 45°C, and their stability, in terms of particle size, dispersion index, and zeta potential was evaluated in different time intervals up to 5 months. Following the changes in particle size is a suitable method to evaluate physical stability. As seen in Figure 3A, the average increase in particle size over a period of 5 months was less than twice the initial average particle size at each temperature. This finding indicated that the particles were not accumulated, and the changes in particle size may be due to the swelling of more surfactant absorptions on nanostructure surface. The obtained zeta potential results were in agreement with these results, confirming the stability of particles. The particle surface charge is one of the important parameters for evaluating physical stability. Higher physical repulsion between particles results in higher physical stability. To sum up, the CUR-NLC-SPIONs showed a high stability in the different conditions and according to Figure 3B, time and temperature did not exert a significant impact on NPs stability.

4.4. Curcumin Entrapment by Magnetic NLC

A standard curve was obtained by measuring the concentration of curcumin in water-tween or ethanol solution at the wavelength of 426 nm. It was used to calculate the amount of curcumin entrapped in or released by CUR-NLC-SPIONs. According to the calibration curve, the accuracy and precision (RSD%) and limit of detection for curcumin analysis were 4.54%, $\pm$ 105.1% and 0.192 μg/mL, respectively.

The amount of curcumin entrapped in CUR-NLC-SPIONs was obtained using Equations 1 and 2. The average for entrapment efficacy (EE) and DL were 99.95 $\pm$ 0.015 % and 3.76 $\pm$ 0.005, respectively. The high EE (more than 99%) for all three samples showed a suitable efficacy of prepared nanostructure for curcumin loading.

4.5. Curcumin Release Study

Figure 4 shows the in vitro curcumin release profile from CUR-NLC-SPIONs at a pH of 7.4. The drug release from CUR-NLC-SPIONs was compared with the release of free drug as the control. Curcumin was released from CUR-NLC-SPIONs in a more controlled release manner compared with the control, and following a controlled drug release for 48 h, the drug release reached a plateau. This finding confirmed the more effectiveness of CUR-NLC-SPIONs to provide sustained release than the control. Moreover, the maximum attainable drug release for free curcumin after 96 h was 60.40%, whereas it was 32.34% for CUR-NLC-SPIONs indicating higher solubility of the curcumin in nanoparticulate platform compared with the free drug.

4.6. MTT Assay

Figure 5 shows the results of MTT assay. The studied cells were treated with the increasing concentrations of CUR-NLC-SPIONs, NLC-SPIONs, and free curcumin for 48, 72, and 96 h. As shown, the cytotoxic effects of the curcumin were increased when loaded on NLC-SPIONs. The calculated IC_{50} of the CUR-NLC-SPIONs on MCF-7 cells after 48, 72, and 96 h exposure was approximately 42.1, 28.4, and 19.9 μg/mL, respectively. Compared with IC_{50} of free curcumin, CUR-NLC-SPIONs had lower IC_{50}s on MCF-7 cells after 72 and 96 h, which can indicate a better solubility and penetration of curcumin with this newly designed nanoformulation. Our data also confirmed the safety of synthesized NLS-SPIONs, since they did not produce toxic effects at studied time periods.

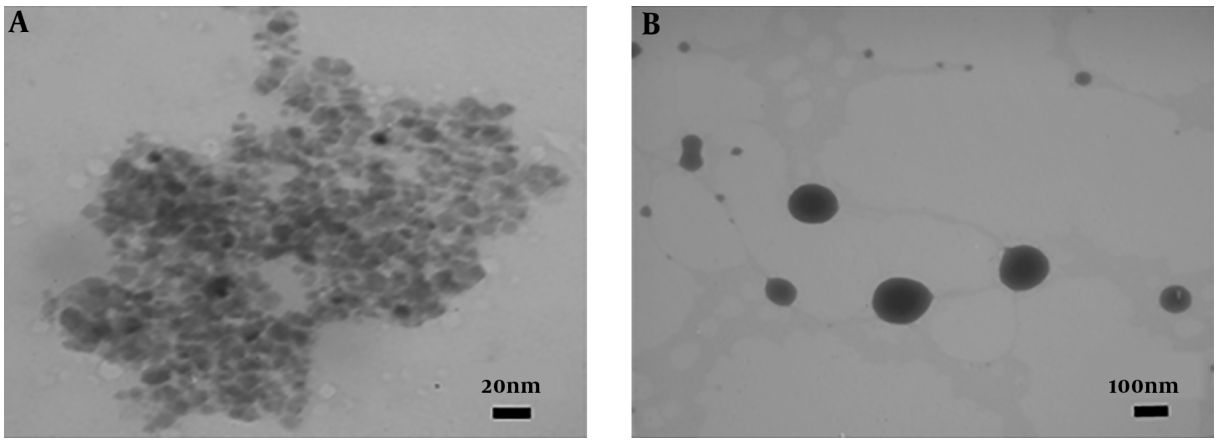

Figure 1. TEM images showing the morphology and distribution of A, SPIONSs, with spherical shape and size about 8 - 10 nm; B, SPIONSs-NLC loaded with curcumin, with a size range of 100 - 150 nm.

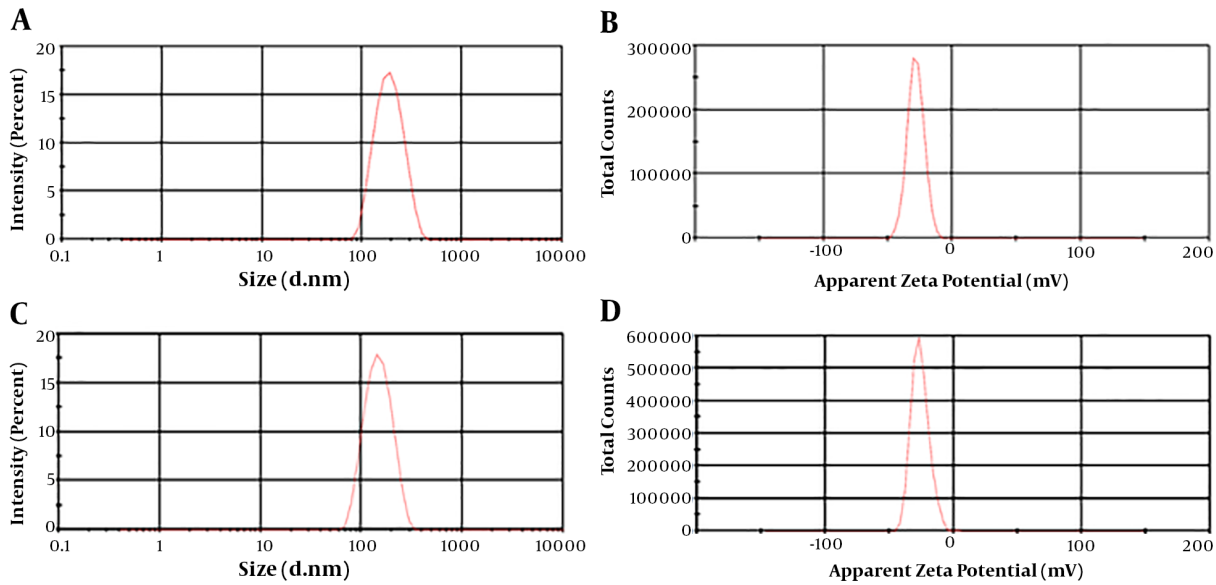

Figure 2. Dynamic light scattering (DLS) results. A, Size and distribution of SPIONs; B, zeta potential of SPIONs; C, size and distribution of CUR-NLC-SPIONs; D, zeta potential of CUR-NLC-SPIONs.

5. Discussion

In this research, for the first time, we described a targeted curcumin delivery system using SPIONs with lipid nanostructured lipid carrier to improve the efficacy of breast cancer treatment. The selected anti-cancer drug in this study, curcumin (diferuloylmethane), has a potent antiproliferative effect against a variety of tumors in vitro through diverse biological properties (25-27). It also increases the antitumor effects of several chemotherapeutic drugs (28, 29) and has some advantages, including vegetable-based, very low side effects, cost-effectiveness, and accessibility (30). However, the therapeutic effects of this compound are limited due to lower aqueous solubility, chemical instability, rapid metabolism and clearance, and poor gastrointestinal absorption (31). To overcome these problems, a nanoparticulate system appears as an optimal solution. Therefore, in the present study, we used SPION incorporated with NLC for targeted delivery of curcumin to the MCF-7 cell line.

At the first, the SPIONs coated with oleic acid were synthesized with the co-precipitation method. The reaction

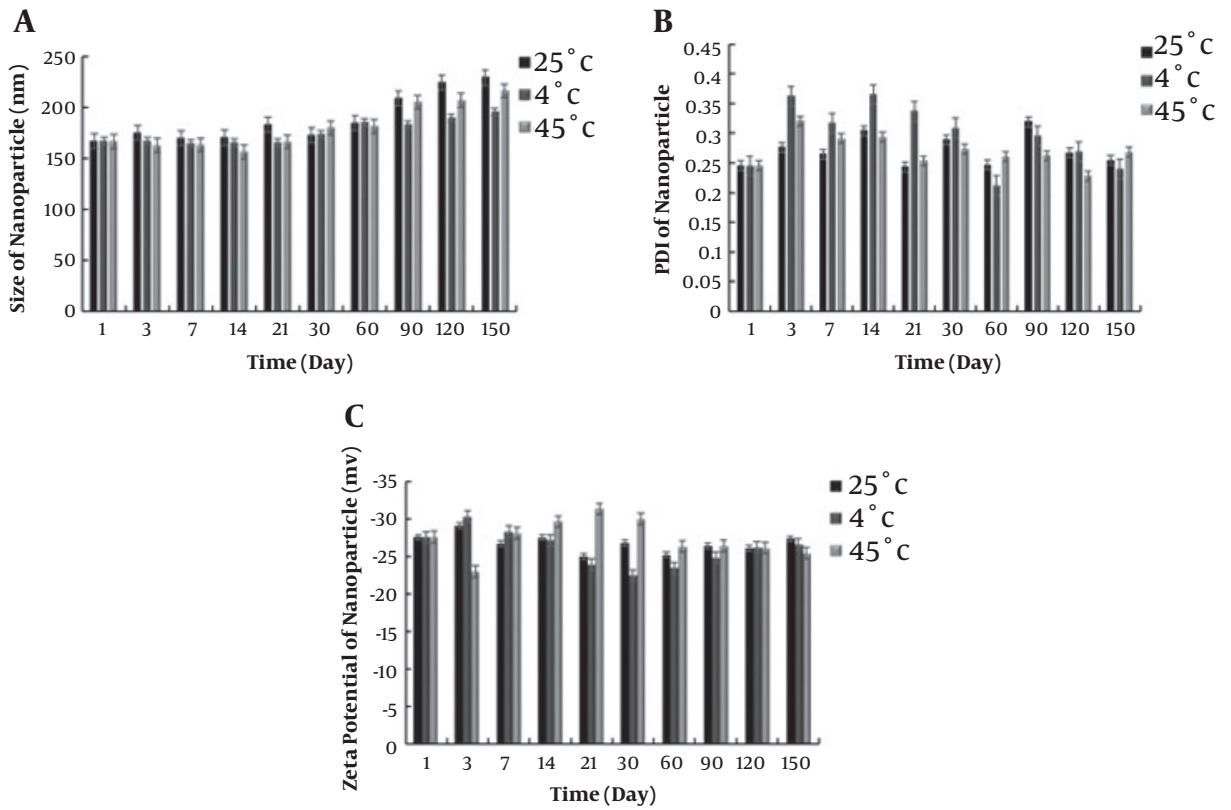

Figure 3. The stability of A, size; B, polydispersity index; and C, zeta potential of CUR-NLC-SPIONs in time intervals up to 5 months and in three temperatures of 25°C, 4°C, and 45°C. Every bar represents the mean value obtained from three samples.

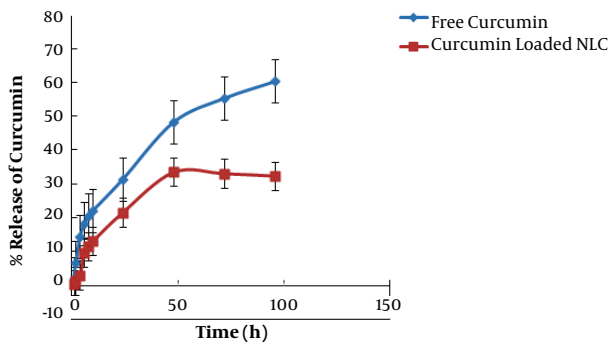

Figure 4. Curcumin release profiles from CUR-NLC-SPIONs at pH = 7.4

was maintained under a nitrogen atmosphere to prevent the SPION oxidation. Oleic acid makes SPIONS to show high magnetization values resulting from diminution of surface spin disorder, and also high crystallinity of SPIONs (32). Hence, the NPs showed an appropriate stability and dispersity in organic solvents due to oleic acid. The size of these NPs was at the range of 8 - 10 nm shown by TEM. The spherical morphology of the NPs and their magnetic properties were also suitable.

In the next step, curcumin was loaded in the SPIONs incorporated with NLCs. Accordingly, solid and liquid lipids were used. Fish oil, as a liquid lipid, has some fatty acids, which their carboxylic groups are deionized after exposure to water, producing a slightly negative charge and resulting in negatively charged NPs that help the stability of them (33). Non-ionic surfactants, i.e. Tween 80 and span 60 were used, because their corresponding steric hindrance further increases the stability of the colloidal dispersion (34).

The successful synthesis of Cur-NLC-SPIONs was investigated by TEM and DLS. The size range obtained by DLS was 166.7 $\pm$ 14.20 nm. Depending on the shape, surface composition, and charge, the size range of NPs is varied (35). Very small-sized NPs (< 5 - 10 nm) are excreted renally (36), however, medium-sized NPs (30 - 150 nm) are widely distributed to the bone marrow, heart, kidney, and stomach (37). Therefore, the size of 166.7 $\pm$ 14.20 nm obtained for

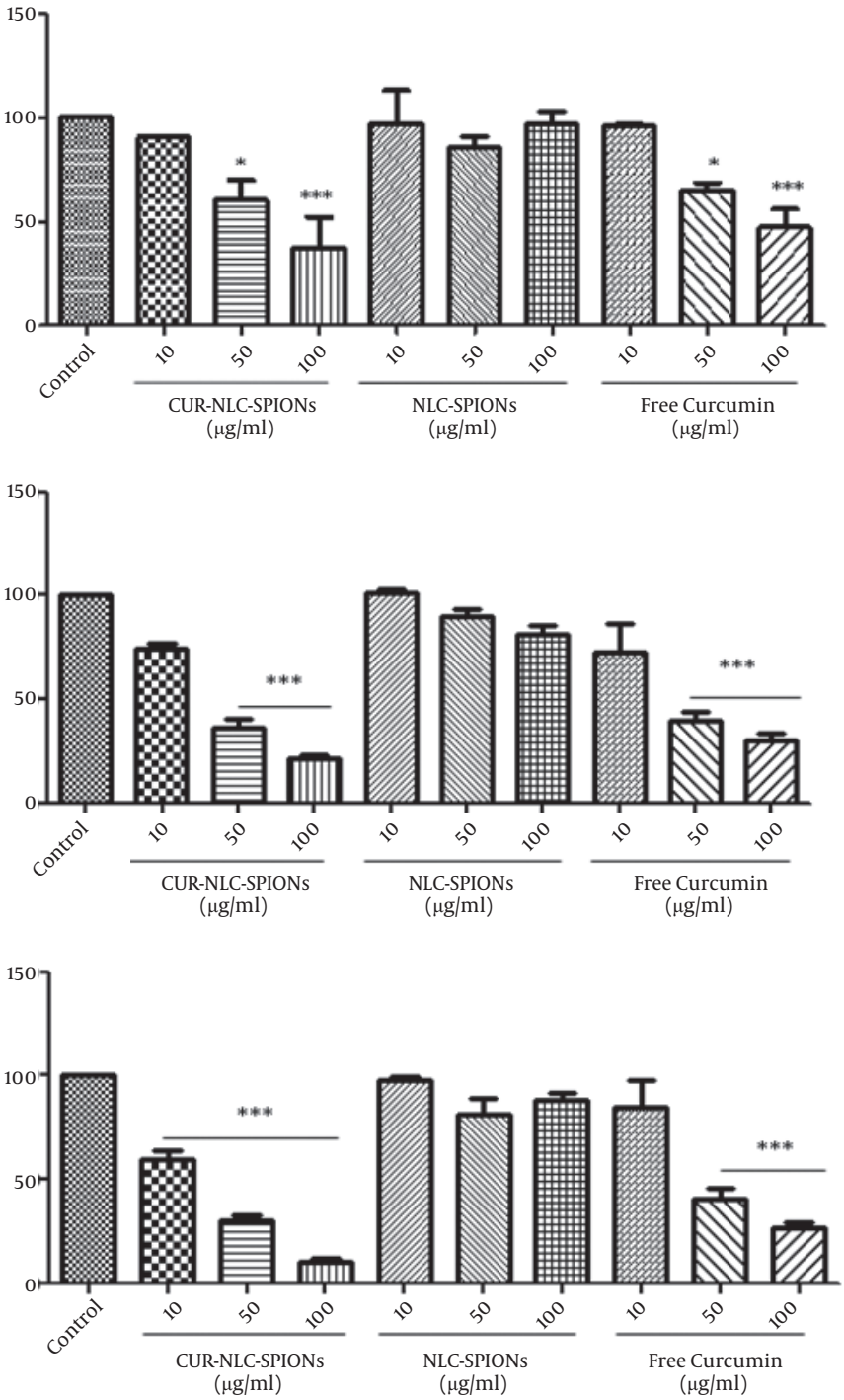

Figure 5. The effect of CUR-NLC-SPIONs on MCF-7 cells. The cells were treated with desired concentrations of the samples and incubated for 48, 72, and 96 h at cell culture incubator. Cell viability was then assessed using MTT method AND presented as a ratio (%) to control group. $^{*}P \leq 0.05$; $^{**}P \leq 0.01$; $^{***}P \leq 0.001$.

Cur-NLC-SPIONs in this study showed a desired potential to distribute in the body and affecting the targeted organ.

The result of TEM and DLS for SPIONs was relatively different. This difference in particle size of TEM and DLS could be due to different causes. It can be explained by a high tendency of SPIONs to aggregate due to magnetic force, particularly in aqueous solution. Besides, the DLS measures the particle size in suspension form, whereas TEM measures size in dried form. Hence, DLS is a better indication of nanoparticle size, along with the PDI. Secondly, TEM provides the data for only a few hundred particles. However, in DLS technique, data is collected from many particles. And another reason can be the placement of SPIONs in the surface of NLC. The zeta potential obtained by DLS was -27.6 $\pm$ 3.83 mV. For an electrostatically stable nanostructure, a minimum zeta potential is $\pm$ 30 mV. Considering the obtained zeta potential of our designed nanostructure, it was suitable (24). PDI is a parameter to define the distribution of the size of NPs population with an acceptable range of 0 - 0.3 nm (38), which it was 0.24 $\pm$ 0.14 for the prepared NPs, indicating the suitable distribution of Cur-NLC-SPIONS.

The storage stability of nano-system was analyzed at three temperatures. The best way to determine the physical stability of NPs is measuring the changes in particle size and surface potentials (39). Surface potentials play an important role in NP stability due to electrostatic repulsion. A higher physical repulsion among particles results in higher physical stability (39). Among three temperatures of 25°C, 4°C and 45°C, the samples stored at 4°C had a greater stability in terms of size. An increase in average particle size over a period of 5 months was very low in two other temperatures. This indicates that particles have not accumulated and slight changes in particle size at 25°C and 45°C groups can be due to the swelling or absorption of the surfactant on the nanostructure surface. PDI and zeta potential of NPs were almost unchanged in three groups at different times and temperatures.

In the next step, the drug loading and in vitro drug release were evaluated. Various factors, such as the physical and chemical structure of the solid matrix, the solubility of the drug or its combination and mixing with melted lipid can affect loading capacity (40). DL% and EE% were determined 3.76% $\pm$ 0.005 and 99.95% $\pm$ 0.015, respectively, indicating an adequate curcumin loading in NPs.

The in vitro release of curcumin from NPs at PH = 7.4 was compared with free drug release and it was observed that the drug release from LNPs had two phases with a slower and gradual rate of releasing in the second phase. The more release rate of drug at the first phase is due to the drug absorbed on the surface of Cur-NLC-SPIONs. This controlled and gradual release of curcumin could result in more lasting effects and higher efficiency in targeted area in vivo. Besides, the free drug can reach toxic doses and due to poor bioavailability and solubility is removed faster from the body and naturally does not have the desired effect. In the present study, gradual curcumin release from designed formulation was obtained, which could result in nontoxic effects and delayed removal from the body. In other words, the half-life of the curcumin could be increased and the need for repeated doses would be eliminated with reduced possible side effects. Our data obtained by cell viability assay showed the stronger cytotoxic effect on MCF-7 cells in a time- and dose-dependent manner, indicating the improvement of pharmacokinetic properties of the curcumin.

5.1. Conclusions

The results of this study showed that the CUR-NLC-SPIONs are suitable carriers as a nano-formulation for targeted therapy of cancer cells by curcumin.

Acknowledgments

This study was extracted from a Pharm. D. thesis by Somayeh Karami.

Footnotes

Authors' Contribution: Somayeh Karami: student, doing synthesis and characterization of SPIONs, writing the draft. Kobra Rostamizadeh: professor: helping with designing the project, helping with checking all synthesis and characterization data, helping with training the student, helping with manuscript preparation. Nasim Shademani: student, doing cell culture experiment. Maliheh Parsa: professor, corresponding author, maneger of the team, designing the project, checking data, preparing and submiting the manu.

Conflict of Interests: The authors declare no conflict of interests.

Ethical Approval: This research was ethically approved by the Ethic Committee, Zanjan University of Medical Sciences, Zanjan, Iran (approval code: IR.ZUMS.RES.1397.360).

Funding/Support: This study was financially supported by the Zanjan University of Medical Sciences, Zanjan, Iran (no.: A-12-929-7).

References

1. DeSantis CE, Ma J, Goding Sauer A, Newman LA, Jemal A. Breast cancer statistics, 2017, racial disparity in mortality by state. *CA Cancer J Clin*. 2017;**67**(6):439–48. doi: 10.3322/caac.21412. [PubMed: 28972651].
2. Siegel RL, Miller KD, Jemal A. Cancer statistics, 2016. *CA Cancer J Clin*. 2016;**66**(1):7–30. doi: 10.3322/caac.21332. [PubMed: 26742998].

3. Liu YL, Chen D, Shang P, Yin DC. A review of magnet systems for targeted drug delivery. *J Control Release*. 2019;**302**:90–104. doi: 10.1016/j.jconrel.2019.03.031. [PubMed: 30946854].
4. Ahmadi N, Rostamizadeh K, Modarresi-Alam AR. Therapeutic anti-inflammatory potential of different formulations based on coenzyme Q10-loaded nanostructured lipid carrier: In vitro, ex vivo, and in vivo evaluations. *Eur J Lipid Scie Technol*. 2018;**120**(11):1800232. doi: 10.1002/ejlt.201800232.
5. Tom G, Philip S, Isaac R, Praseetha PK, Jiji SG, Asha VV. Preparation of an efficient and safe polymeric-magnetic nanoparticle delivery system for sorafenib in hepatocellular carcinoma. *Life Sci*. 2018;**206**:10–21. doi: 10.1016/j.lfs.2018.04.046. [PubMed: 29709652].
6. Shaghaghi B, Khoee S, Bonakdar S. Preparation of multifunctional Janus nanoparticles on the basis of SPIONs as targeted drug delivery system. *Int J Pharm*. 2019;**559**:1–12. doi: 10.1016/j.ijpharm.2019.01.020. [PubMed: 30664992].
7. Cicha I, Scheffler L, Ebenau A, Lyer S, Alexiou C, Goppelt-Struebe M. Mitoxantrone-loaded superparamagnetic iron oxide nanoparticles as drug carriers for cancer therapy: Uptake and toxicity in primary human tubular epithelial cells. *Nanotoxicology*. 2016;**10**(5):557–66. doi: 10.3109/17435390.2015.1095364. [PubMed: 26468004].
8. Mancarella S, Greco V, Baldassarre F, Vergara D, Maffia M, Leporatti S. Polymer-coated magnetic nanoparticles for curcumin delivery to cancer cells. *Macromol Biosci*. 2015;**15**(10):1365–74. doi: 10.1002/mabi.201500142. [PubMed: 26085082].
9. Jadhav NR, Powar T, Shinde S, Nadaf S. Herbal nanoparticles: A patent review. *Asian J Pharm*. 2014;**8**(1):58. doi: 10.4103/0973-8398.134101.
10. Kar S, Kundu B, Reis RL, Sarkar R, Nandy P, Basu R, et al. Curcumin ameliorates the targeted delivery of methotrexate intercalated montmorillonite clay to cancer cells. *Eur J Pharm Sci*. 2019;**135**:91–102. doi: 10.1016/j.ejps.2019.05.006. [PubMed: 31078644].
11. Ayubi M, Karimi M, Abdpour S, Rostamizadeh K, Parsa M, Zamani M, et al. Magnetic nanoparticles decorated with PEGylated curcumin as dual targeted drug delivery: Synthesis, toxicity and biocompatibility study. *Mater Sci Eng C Mater Biol Appl*. 2019;**104**:109810. doi: 10.1016/j.msec.2019.109810. [PubMed: 31499939].
12. Gomez-Bougie P, Halliez M, Maiga S, Godon C, Kervoelen C, Pellat-Deceunynck C, et al. Curcumin induces cell death of the main molecular myeloma subtypes, particularly the poor prognosis subgroups. *Cancer Biol Ther*. 2015;**16**(1):60–5. doi: 10.4161/15384047.2014.986997. [PubMed: 25517601]. [PubMed Central: PMC4622499].
13. Kurien BT, Dorri Y, Scofield RH. Spicy SDS-PAGE gels: Curcumin/turmeric as an environment-friendly protein stain. *Methods Mol Biol*. 2012;**869**:567–78. doi: 10.1007/978-1-61779-821-4_51. [PubMed: 22585522].
14. Massart R, Cabuil V. [Effect of some parameters on the formation of colloidal magnetite in alkaline-medium-yield and particle-size contro]. *J Chim Phys*. 2017;**84**:967–73. French. doi: 10.1051/jcp/1987840967.
15. Zhu X, Deng X, Lu C, Chen Y, Jie L, Zhang Q, et al. SPIO-loaded nanostructured lipid carriers as liver-targeted molecular T2-weighted MRI contrast agent. *Quant Imaging Med Surg*. 2018;**8**(8):770–80. doi: 10.21037/qims.2018.09.03. [PubMed: 30306057]. [PubMed Central: PMC6177360].
16. Saedi A, Rostamizadeh K, Parsa M, Dalali N, Ahmadi N. Preparation and characterization of nanostructured lipid carriers as drug delivery system: Influence of liquid lipid types on loading and cytotoxicity. *Chem Phys Lipids*. 2018;**216**:65–72. doi: 10.1016/j.chemphyslip.2018.09.007. [PubMed: 30219661].
17. Ng WK, Saiful Yazan L, Yap LH, Wan Nor Hafiza WA, How CW, Abdullah R. Thymoquinone-loaded nanostructured lipid carrier exhibited cytotoxicity towards breast cancer cell lines (MDA-MB-231 and MCF-7) and cervical cancer cell lines (HeLa and SiHa). *Biomed Res Int*. 2015;**2015**:263131. doi: 10.1155/2015/263131. [PubMed: 25632388]. [PubMed Central: PMC4303008].
18. Amanlou N, Parsa M, Rostamizadeh K, Sadighian S, Moghaddam F. Enhanced cytotoxic activity of curcumin on cancer cell lines by incorporating into gold/chitosan nanogels. *Mater Chem Phys*. 2019;**226**:151–7. doi: 10.1016/j.matchemphys.2018.12.089.
19. Arora S; Wahajuddin. Superparamagnetic iron oxide nanoparticles: Magnetic nanoplatforms as drug carriers. *Int J Nanomedicine*. 2012;**7**:3445–71. doi: 10.2147/IJN.S30320. [PubMed: 22848170]. [PubMed Central: PMC3405876].
20. Liu D, Liu Z, Wang L, Zhang C, Zhang N. Nanostructured lipid carriers as novel carrier for parenteral delivery of docetaxel. *Colloids Surf B Biointerfaces*. 2011;**85**(2):262–9. doi: 10.1016/j.colsurfb.2011.02.038. [PubMed: 21435845].
21. Chen Y, Yang X, Zhao L, Almásy L, Garamus VM, Willumeit R, et al. Preparation and characterization of a nanostructured lipid carrier for a poorly soluble drug. *Colloids Surf A*. 2014;**455**:36–43. doi: 10.1016/j.colsurfa.2014.04.032.
22. Kawadkar J, Pathak A, Kishore R, Chauhan MK. Formulation, characterization and in vitro-in vivo evaluation of flurbiprofen-loaded nanostructured lipid carriers for transdermal delivery. *Drug Dev Ind Pharm*. 2013;**39**(4):569–78. doi: 10.3109/03639045.2012.686509. [PubMed: 22639934].
23. Lai CW, Low FW, Tai MF, Abdul Hamid SB. Iron oxide nanoparticles decorated oleic acid for high colloidal stability. *Adv Polym Technol*. 2018;**37**(6):1712–21. doi: 10.1002/adv.21829.
24. Muller R. *Zetapotential und partikelladung±kurze theorie, praktische meudurchfu ehrung, daten interpretation*. Germany: Wissenschaftliche Verlagsgesellschaft, Stuttgart; 1996.
25. Arbiser JL, Klauber N, Rohan R, van Leeuwen R, Huang MT, Fisher C, et al. Curcumin is an in vivo inhibitor of angiogenesis. *Mol Med*. 1998;**4**(6):376–83. [PubMed: 10780880]. [PubMed Central: PMC2230271].
26. Aggarwal BB, Kumar A, Bharti AC. Anticancer potential of curcumin: preclinical and clinical studies. *Anticancer Res*. 2003;**23**(1A):363–98. [PubMed: 12680238].
27. Li L, Braiteh FS, Kurzrock R. Liposome-encapsulated curcumin: In vitro and in vivo effects on proliferation, apoptosis, signaling, and angiogenesis. *Cancer*. 2005;**104**(6):1322–31. doi: 10.1002/cncr.21300. [PubMed: 16092118].
28. Chan MM, Fong D, Soprano KJ, Holmes WF, Heverling H. Inhibition of growth and sensitization to cisplatin-mediated killing of ovarian cancer cells by polyphenolic chemopreventive agents. *J Cell Physiol*. 2003;**194**(1):63–70. doi: 10.1002/jcp.10186. [PubMed: 12447990].
29. Bava SV, Puliyappadamba VT, Deepti A, Nair A, Karunagaran D, Anto RJ. Sensitization of taxol-induced apoptosis by curcumin involves down-regulation of nuclear factor-kappaB and the serine/threonine kinase Akt and is independent of tubulin polymerization. *J Biol Chem*. 2005;**280**(8):6301–8. doi: 10.1074/jbc.M410647200. [PubMed: 15590651].
30. Bharat BA, Young-Joon S, Shishir S. *The molecular targets and therapeutic uses of curcumin in health and disease*. **595**. Germany: Springer Science and Business Media; 2007. doi: 10.1007/978-0-387-46401-5_1.
31. Anand P, Kunnumakkara AB, Newman RA, Aggarwal BB. Bioavailability of curcumin: problems and promises. *Mol Pharm*. 2007;**4**(6):807–18. doi: 10.1021/mp700113r. [PubMed: 17999464].
32. de Montferrand C, Hu L, Lalatonne Y, Lièvre N, Bonnin D, Brioude A, et al. SiO2 versus chelating agent@ iron oxide nanoparticles: interactions effect in nanoparticles assemblies at low magnetic field. *J Sol-Gel Sci Technol*. 2014;**73**(3):572–9. doi: 10.1007/s10971-014-3526-y.
33. Huang ZR, Hua SC, Yang YL, Fang JY. Development and evaluation of lipid nanoparticles for camptothecin delivery: A comparison of solid lipid nanoparticles, nanostructured lipid carriers, and lipid emulsion. *Acta Pharmacol Sin*. 2008;**29**(9):1094–102. doi: 10.1111/j.1745-7254.2008.00829.x. [PubMed: 18718178].
34. Das S, Ng WK, Tan RB. Are nanostructured lipid carriers (NLCs) better than solid lipid nanoparticles (SLNs): Development, characterizations and comparative evaluations of clotrimazole-loaded SLNs and NLCs? *Eur J Pharm Sci*. 2012;**47**(1):139–51. doi: 10.1016/j.ejps.2012.05.010.

[PubMed: 22664358].
35. Reddy LH, Arias JL, Nicolas J, Couvreur P. Magnetic nanoparticles: Design and characterization, toxicity and biocompatibility, pharmaceutical and biomedical applications. *Chem Rev*. 2012;**112**(11):5818–78. doi: 10.1021/cr300068p. [PubMed: 23043508].
36. Choi HS, Liu W, Misra P, Tanaka E, Zimmer JP, Itty Ipe B, et al. Renal clearance of quantum dots. *Nat Biotechnol*. 2007;**25**(10):1165–70. doi: 10.1038/nbt1340. [PubMed: 17891134]. [PubMed Central: PMC2702539].
37. Veiseh O, Gunn JW, Zhang M. Design and fabrication of magnetic nanoparticles for targeted drug delivery and imaging. *Adv Drug Deliv Rev*. 2010;**62**(3):284–304. doi: 10.1016/j.addr.2009.11.002. [PubMed: 19909778]. [PubMed Central: PMC2827645].
38. Olbrich C, Muller RH. Enzymatic degradation of SLN-effect of surfactant and surfactant mixtures. *Int J Pharm*. 1999;**180**(1):31–9. doi: 10.1016/s0378-5173(98)00404-9. [PubMed: 10089289].
39. Mitri K, Shegokar R, Gohla S, Anselmi C, Muller RH. Lipid nanocarriers for dermal delivery of lutein: Preparation, characterization, stability and performance. *Int J Pharm*. 2011;**414**(1-2):267–75. doi: 10.1016/j.ijpharm.2011.05.008. [PubMed: 21596122].
40. Muller RH, Mader K, Gohla S. Solid lipid nanoparticles (SLN) for controlled drug delivery - a review of the state of the art. *Eur J Pharm Biopharm*. 2000;**50**(1):161–77. doi: 10.1016/s0939-6411(00)00087-4. [PubMed: 10840199].